Ecological Informatics 71 (2022) 101776

Contents lists available at ScienceDirect

Ecological Informatics

journal homepage: www.elsevier.com/locate/ecolinf

Vegetation coverage changes driven by a combination of climate change and human activities in Ethiopia, 2003–2018

Shengjie Yang [a,b], Shuai Song [a,d,*], Fadong Li [c,d], Mingzhao Yu [a], Guangming Yu [b], Qiuying Zhang [e], Haotian Cui [a], Rui Wang [a], Yanqi Wu [a]

[a] State Key Laboratory of Urban and Regional Ecology, Research Center for Eco-Environmental Sciences, Chinese Academy of Sciences, Beijing 100085, China
[b] Key Laboratory for Geographical Process Analysis & Simulation of Hubei Province/College of Urban and Environmental Sciences, Central China Normal University, Wuhan 430079, China
[c] Key Laboratory of Ecosystem Network Observation and Modeling, Institute of Geographic Sciences and Natural Resources Research, Chinese Academy of Sciences, Beijing 100101, China
[d] College of Resources and Environment, University of Chinese Academy of Sciences, Beijing 100049, China
[e] Chinese Research Academy of Environmental Sciences, Beijing 100012, China

ARTICLE INFO

Keywords:
Fractional vegetation coverage
Ethiopia
Climate change
Human activity
Spatiotemporal dynamic

ABSTRACT

Climate change often leads to the vulnerability of vegetation cover, while the impact of human activities on vegetation cover is undoubtedly more complex in this context, especially in Ethiopia. This paper analyzed the spatiotemporal dynamics of vegetation growth in Ethiopia from 2003 to 2018 by the enhanced vegetation index (EVI) based on different time scales and explored the coefficient of variation and driving factors of the fractional vegetation coverage (FVC). The results indicated that the EVI mainly presents a "double peak" pattern, with large spatiotemporal differences between quarters and months in Ethiopia. The FVC increased by 0.0005 per year, but vegetation showed a browning trend after 2013. The FVC degraded area accounted for 43.9% of the total area, of which the significantly degraded area accounted for 7.51% due to human activities, mainly in northern, central, and southern Ethiopia. The effects of precipitation and maximum temperature on vegetation differed on time scales. Spatially, the vegetation on the northwest side of the Main Ethiopian Rift Valley (MERV) was dominated by a combination of maximum temperature and precipitation, while vegetation on the southeast side of MERV was mainly influenced by precipitation. However, the spatial overlay analysis with degraded and healthy vegetation zones revealed that human activities were the key driver of vegetation cover change rather than climate change. This study provides support for further development of vegetation health conservation policies in Ethiopia and monitoring of vegetation dynamics in other countries around the world.

1. Introduction

Vegetation is a general term for all surface plant communities, including forests, grasslands, shrubs, etc., and is a key factor in the Earth's terrestrial ecosystem (Arneth, 2015). Vegetation communities are the places where many animals and microorganisms depend, among which forest and grassland ecosystems are important carbon pools (Palmer, 2021). In addition, vegetation has a wide range of socioeconomic benefits, providing a continuous supply of wood and energy for human beings, supporting human livestock development, and providing an ecological barrier to food security.

As a major component of land cover, vegetation cover has been one of the core elements of global change research. Vegetation cover-related studies are mainly combined with remote sensing estimation, vegetation structure function, biodiversity, ecosystem services, dynamic evolution and drivers, scenario simulation, interaction, and urban expansion-socioeconomic-vegetation change correlation analysis (Shen et al., 2021; Swain et al., 2017; Zhang et al., 2021a; Zhou et al., 2022). The development of remote sensing technology provides a wide range of data support for monitoring vegetation dynamics. In recent years, many researchers have enriched this field of study at different spatial scales, including the global scale (Cao et al., 2021; Miralles et al., 2017), continental scale (Cannone et al., 2021; Guo et al., 2018), national scale, and regional scale (Li et al., 2020; Thompson et al., 2021). Among them,

* Corresponding author at: State Key Laboratory of Urban and Regional Ecology, Research Center for Eco-Environmental Sciences, Chinese Academy of Sciences, No.18, Shuangqing Road, Haidian, Beijing 100085, China.
E-mail address: shuaisong@rcees.ac.cn (S. Song).

https://doi.org/10.1016/j.ecoinf.2022.101776
Received 15 June 2022; Received in revised form 10 August 2022; Accepted 11 August 2022
Available online 18 August 2022

numerous studies have shown climate change and human activities are generally considered to be the main drivers of vegetation cover change (Ebrahimi Khusfi and Zarei, 2020; Naeem et al., 2020). The flexibility to identify and quantify the effects of these factors on vegetation cover has been the focus of many researchers (Shi et al., 2021; Zhang et al., 2013). Piao et al. (2015) used an ecosystem model to identify the most likely causes of greening trends in China and concluded that climate change had a negative impact on vegetation greening in arid and semi-arid regions.

Unlike the effects of climate change on vegetation cover, the effects of human activities on regional vegetation cover are usually multifaceted and complex due to their close dependence on vegetation resources. Some recent studies have shown that ecological reforestation, grass restoration projects, and grazing ban policies usually have positive impacts on vegetation cover, while indiscriminate logging, mountain fires, urban expansion, and mineral extraction will squeeze the growth space of vegetation cover and eventually lead to the degradation of vegetation cover (Feng et al., 2020; Kumar et al., 2017; Remy et al., 2017). Fractional vegetation coverage (FVC) is the ratio of the vertical projected area of vegetation to the total ground area (Gitelson et al., 2002; Wu et al., 2014), and is an important indicator to reflect the quality of the ecological environment (Gitelson et al., 2002; Li et al., 2014; Wu et al., 2014). Vegetation indices (VIs) are commonly used to estimate FVC, such as the normalized difference vegetation index (NDVI), the enhanced vegetation index (EVI) (Qiu et al., 2013; Dutta et al., 2015). NDVI shows saturation in dense vegetation canopies, including forests, while the EVI improves the sensitivity to dense vegetation, reduces the influence of atmospheric and soil backgrounds, and has a stronger ability to distinguish vegetation (Liu and Huete, 1995; Rouse et al., 1974). Several studies monitored the dynamic changes in vegetation cover and its relationship with topography in the wind-sand source area and the Pisha Sandstone area based on the FVC (Wang et al., 2020; Yang et al., 2015). This indicates that FVC has the equivalent or better ability to quantify vegetation cover change. Natural vegetation cover change is a subtle and long process. Describing vegetation cover change dynamically from multiple dimensions is the core of this paper's research.

The degradation of vegetated ecosystems may further lead to desertification, an increase in greenhouse gases, and even a range of social problems, such as reduced agricultural production and increased poverty (Gebru et al., 2020; Ortiz-Bobea et al., 2021). Identifying the degradation status of vegetation under the influence of climate change and human activities is a critical task to protect terrestrial vegetation ecosystems.

Ethiopia is a typical developing country and is deeply affected by climate change (Shuai et al., 2018). Due to global changes, the country has experienced a 20% decrease in precipitation since 1960, with a substantial increase in the frequency of droughts (Beyene, 2015). Ethiopia's economic development is highly dependent on natural resources (Adem et al., 2020). Unsustainable resource extraction will undoubtedly aggravate vegetation degradation and affect vegetation ecosystem resilience. To promote the healthy development of vegetation ecosystems in Ethiopia, determining the spatial distribution of climate change and human activities' impacts on vegetation cover, identifying the main drivers, and distinguishing between degraded vegetation zones and healthy vegetation zones are the focus of current work. Previous studies showed that the main factor affecting the degradation of vegetation cover in the Buno Bedelle zone, Oromia Region of Ethiopia, was resettlement (Abera et al., 2020). Another study showed that urbanization was the main cause for the change in Addis Ababa's vegetation cover (Arsiso et al., 2018). Hence, the anthropogenic stressors on vegetation cover differently in different regions. In the context of global warming, the impact of human activities on vegetation cover is likely to be more profound. Although Ethiopia has achieved remarkable economic development since the turn of the 21st century, it has also profoundly altered the surface vegetation landscape. However, the current scale of vegetation dynamics studies in Ethiopia is dominated by local area-based case studies, and the understanding of vegetation response mechanisms to climate change and human activities is still limited, with lack of national-scale studies.

Therefore, the nationwide analysis of the response of vegetation cover to climate change and human activities is critical to improve the ecological resilience of the country's vegetation and to identify sources of disturbance. The objectives of the study were to (1) answer the basic characteristics of interannual, quarterly, and monthly EVI succession in Ethiopia from 2003 to 2018; (2) construct a 16-year FVC dataset and visualized the development status (healthy and degraded) of vegetation cover; (3) analyze the interannual and monthly correlation between climate factors, human activities, and FVC to reveal the spatial distribution zones of the impact of human activities on FVC; and (4) discuss the driving factors of vegetation cover change and provide a new perspective on the dynamic monitoring and the conservation of vegetation cover.

2. Materials and methods

2.1. Study area

Ethiopia is located in the center of the Horn of Africa and has a total area of approximately 1.14 million km^2 (Fig. S1 (a)). The topography of the country is peculiar, ranging from the Afar Depression (−197 m below sea level) in the east to the World Heritage Mountains (4000 m above sea level) in the north, and its highlands are divided into the northwest and southeast plateaus by the East African Rift Valley, known as the “Roof of Africa” (Asefa et al., 2020). The average precipitation is 838.84 mm and the average temperature is 30.67 °C in Ethiopia. Precipitation in Ethiopia is affected by the Pacific climate system thousands of miles away, especially in the central and central-eastern Pacific near the equator (Funk et al., 2016). The overall population density of Ethiopia is low, mostly concentrated in the plateau (Amsalu and Gebremichael, 2010). Ethiopia is dominated by rain-fed agriculture. Many households across the country are predominantly renting land, which can result in the indiscriminate use of land and make vegetation cover tend to fragment.

2.2. Data and processing

Annual and quarterly EVI calculations were completed based on the MOD13Q1 product, a global 250 m resolution 16-d synthetic vegetation index product. The data version is V006, with a total of 368 images from 2003 to 2018 and 4 images downloaded for January and February 2019. The calculation of monthly EVI was performed based on the MOD13A3 product, with a total of 192 images. The dataset has a spatial resolution of 1 km and is based on a 16-d synthetic product of the same resolution by a weighted-average temporal synthetic algorithm. EVI data was obtained by the AppEEARS (https://lpdaacsvc.cr.usgs.gov/appeears/). Monthly, annual precipitation and maximum temperatures were derived from the TerraClimate raster dataset, with a resolution of approximately 0.04° × 0.04° (Abatzoglou et al., 2018) (http://thredds.northwestknowledge.net:8080). The DEM was obtained from the 4th version of SRTM digital elevation data (Jarvis et al., 2008), and the land use data was from GLC_FCS30–2010 (Zhang et al., 2021b).

Based on the natural breakpoint method and land use data (Fig. S1 (b)), the FVC was divided into four levels, namely, 0–0.2 for poor coverage, 0.2–0.45 for low coverage, 0.45–0.75 for middle coverage, and 0.75 to 1 for high coverage. In order to ensure the consistency of spatial resolution between EVI and climatic factor data, the resolution resampling was carried out on this data. It should be noted that the mean annual maximum temperature (MAMaxTemp) and mean annual precipitation (MAPpt) refer to the arithmetic average of the monthly data month by month during the year. The mean monthly maximum temperature (MMMaxTemp) and mean monthly precipitation (MMPpt) are the average values for the same months during the study period.

2.3. Dimidiate pixel and center of gravity migration models

The dimidiate pixel model is a practical remote sensing estimation model that assumes that the surface of an image element consists of a vegetated part and a nonvegetated part. The equation of the dimidiate pixel model is (Gao et al., 2020):

$$FVC = (EVI - EVI_{soil}) / (EVI_{veg} - EVI_{soil}) \quad (1)$$

where EVI_{soil} is the EVI value of completely bare soil or no vegetation cover area (EVI_{min}), and EVI_{veg} represents the EVI value of a completely vegetation cover pixel, i.e., the EVI value of pure vegetation pixel (EVI_{max}).

The gravity center migration model was used to quantify the migration direction and distance of different FVC. The equation is (Fu et al., 2016):

$$X = \sum_{i=1}^{n}(C_i \times X_i) \Big/ \sum_{i=1}^{n} C_i \quad (2)$$

$$Y = \sum_{i=1}^{n}(C_i \times Y_i) \Big/ \sum_{i=1}^{n} C_i \quad (3)$$

where X and Y denote the latitude and longitude coordinates of the center of gravity of the FVC distribution, respectively; C_i denotes the area of the ith vegetation image element, and X_i and Y_i denote the latitude and longitude coordinates of the center of gravity of the ith vegetation image element, respectively.

2.4. The coefficient of variation and maximum value composite methods

The coefficient of variation (CV) was a quantification of the degree of dispersion of data points around the mean in a data series and was used to measure the response to interannual fluctuations in vegetation cover (He et al., 2021). The maximum value composite (MVC) method can effectively eliminate the effects of atmospheric scattering, cloud cover and solar altitude angle on remote sensing image values, and was used in data reconstruction (Holben, 1986). In this study, EVI data of different time scales was obtained based on MVC method.

2.5. Sen's slope and Mann-Kendall test

Sen's slope is the median of the calculated series and is often used to determine the magnitude of the rise and fall of the trend change in time series data (Sen, 1968). The Mann-Kendall (MK) test has no requirements for the distribution of the series and is not sensitive to outliers, and the use of this method can complete the test for the significance of the trend of the series (Kendall, 1948; Mann, 1945). Data pre-whitening was performed prior to the MK test.

2.6. Correlation and residual trend analysis methods

The correlation between FVC and climate factors (maximum temperature, precipitation) in Ethiopia from 2003 to 2018 was analyzed per pixel using the Pearson correlation coefficient, and the significance was revealed using the f-test. The residual trend (RESTREND) method was used to analyze trends in the impact of human activities on FVC (Ge et al., 2021).

3. Results

3.1. Spatiotemporal variability characteristics for EVI

3.1.1. Spatiotemporal variation of interannual EVI

An overall slow growth trend of the EVI was found, with a linear growth rate of 0.04%/a (Fig. 1 (a)). The highest value of EVI was reached in 2013, while the lowest value occurred in 2009. Meanwhile, the interannual values were highly variable and characterized by irregular fluctuations of sawtooth shape. This reflects the variability and complexity of EVI influencing factors in the study area. The spatial conversion of the EVI was relatively stable during the study period but with obvious spatial heterogeneity (Fig. 2 (a)), showing a decreasing

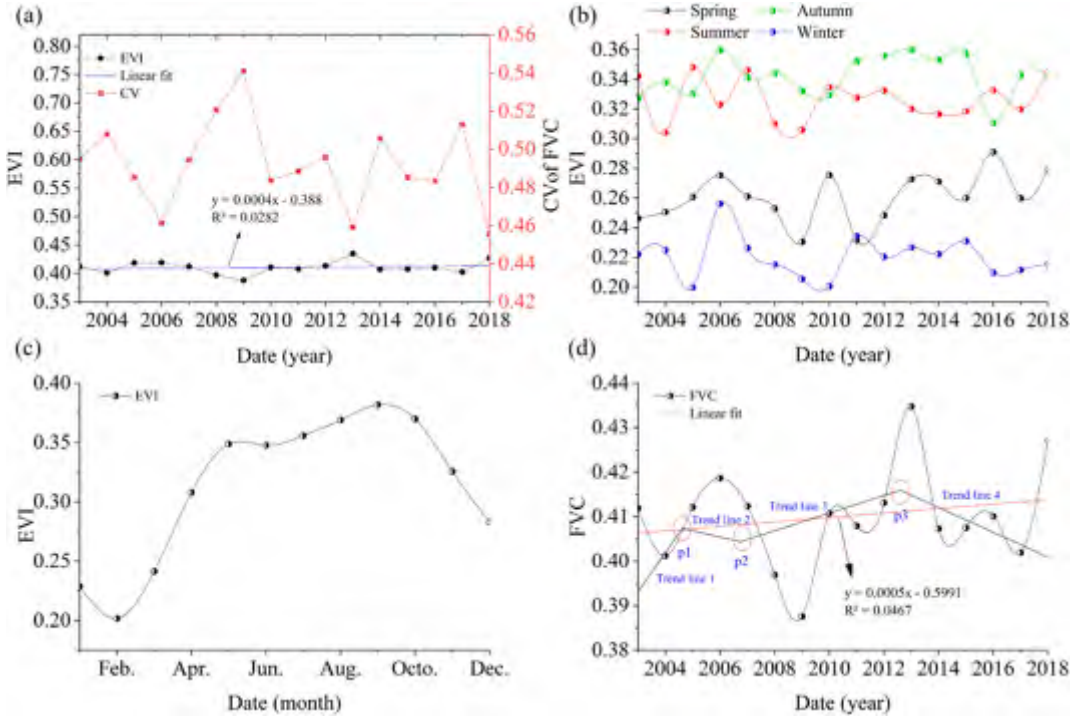

Fig. 1. Annual EVI and CV value of FVC (a), quarterly (spring, summer, autumn, and winter) EVI (b), monthly EVI (c), annual FVC and its change-points (p1, p2, and p3 points) (from 2003 to 2018) (d).

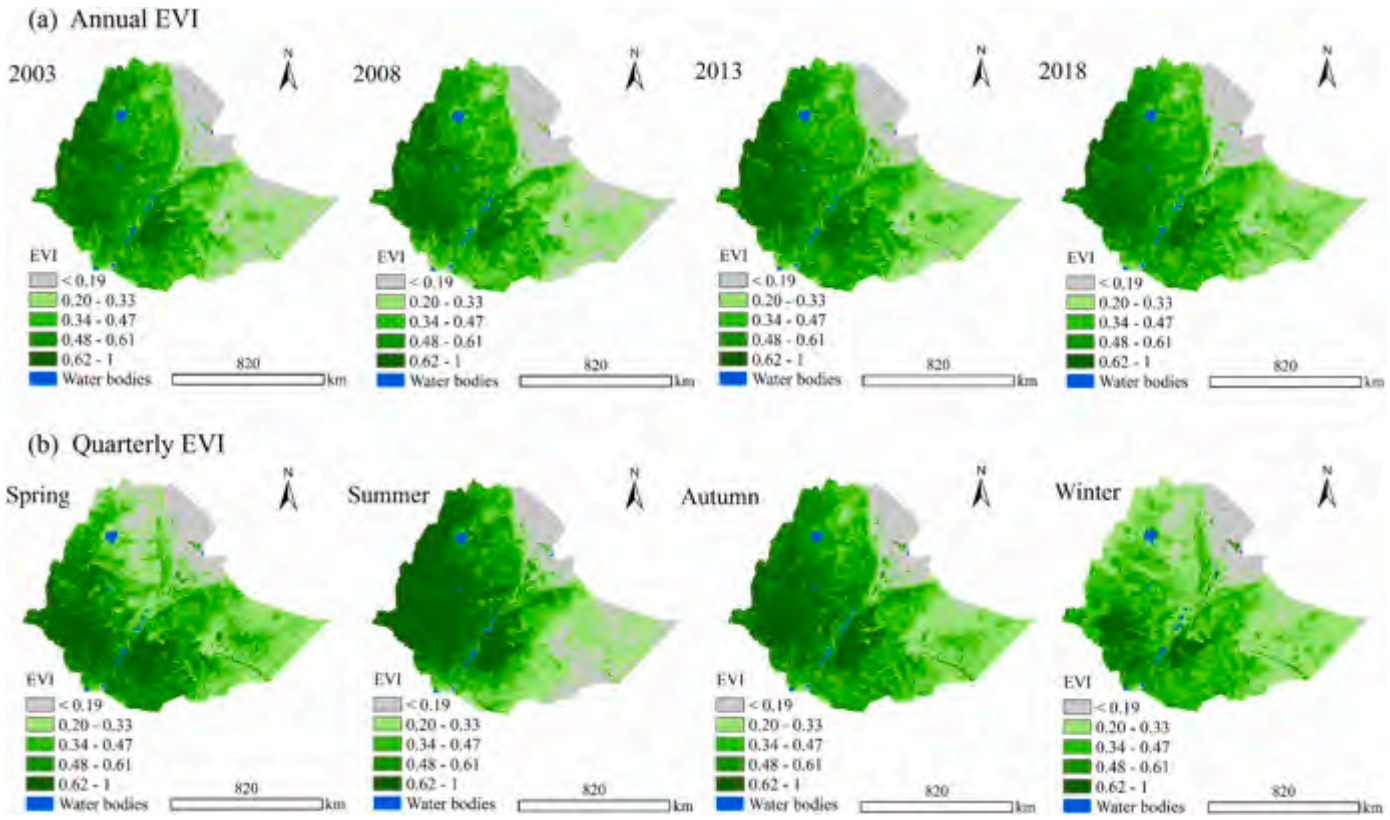

Fig. 2. The spatial distribution of annual (2003, 2008, 2013, 2018) EVI (a) and quarterly (spring, summer, autumn, and winter) EVI (b) in Ethiopia.

trend from northwest to southeast.

3.1.2. Temporal differences in quarterly EVI

Fig. 1 (b) shows that the winter EVI is the lowest in the same year, fluctuating back and forth between 0.199 and 0.256. The interannual variation maintained a balanced and cyclical trend of EVI increase and decrease in winter, except for 2006, when the EVI peaked. The EVI had a slowly increasing trend (plant growth period) from winter to spring. Comparing the EVI in summer and autumn, we found that the overall trend of the EVI was relatively stable, but the fluctuations showed long-term staggered increases or decreases in summer and autumn. Specifically, the EVI ranking was autumn (5.67) > summer (5.5) > spring (4.92) > winter (3.29).

High values of quarterly EVI were generally distributed in the west-central, northwestern, and southwestern parts of Ethiopia, while low values were mainly distributed in the northeast, followed by the southeast (Fig. 2 (b)). The nonvegetated bare land was concentrated in the northeast, and its quarterly EVI showed an overall decreasing trend from the northwest to the northeast. In the transition from spring to summer, the EVI increased substantially in the northeastern Amhara and Tigray regions, while it decreased substantially in the southwestern Somali region. The average altitude of the Midwest highlands of Ethiopia is 2500–3000 m, dominated by rainforest vegetation, resulting in an increase in the EVI in this region. During the transition from summer to autumn, this increasing trend was reversed, and the area of high EVI decreased. The EVI increased in the southeast, mainly in the lowlands, indicating that the seasonal variation in phenology varied substantially among different plant cover types. In summary, the spatial distribution of the EVI in Ethiopia varied substantially with the seasons, and different changing trends were found in the uplands and lowlands.

3.1.3. Temporal differences in monthly EVI

The EVI reached its lowest value at 0.2 in February (Fig. 1 (c)). After February, the EVI increased at a faster rate until May, when it reached a small peak (0.34). After June, the EVI increased at a slow rate until September, when it reached the peak of the year (0.38). EVI decreased rapidly after September. This reflected the overall phenological characteristics of the vegetation in the study area. Overall, the year-round variation in the EVI in Ethiopia showed a “double peak” pattern.

3.2. Dynamic change of FVC

3.2.1. CV of FVC

The interannual variation coefficients of FVC were divided into five grades: strong fluctuation area, moderate fluctuation area, slight fluctuation area, relatively stable area, and stable area. The results showed that the mean CV of the study area ranged from 0.45 to 0.55, with substantial interannual fluctuations (Fig. 1 (a)). The CV peaked in 2009, indicating that the FVC was strongly disturbed in 2009. Fig. 3 (a) shows that the FVC in the northwest and southwest of the study area was in a stable state, with an area of 348,700 km^2, accounting for 30.38% of the total area. The strong fluctuation area was mainly located in the northeastern part of the Afar region. The moderate fluctuation area was mainly located at the border of the Afar and Tigray states, as well as in southwestern Ethiopia.

3.2.2. FVC grading and spatiotemporal evolution

According to the statistics of FVC levels (Fig. S2), the study area was mainly dominated by middle and high coverage. From 2003 to 2018, the middle coverage increased by 4.01%, and the low coverage decreased by 2.19%. The high coverage remained unchanged at about 32%, which indicated that the overall vegetation cover status was relatively stable. The center of gravity migrated most obviously in the poor coverage, followed by the middle coverage. The high coverage in southwestern Ethiopia had the least migration span, with the direction of “southwest–southeast–west” (Fig. 3 (b)).

The highest FVC was 0.43 in 2013, and the lowest value was 0.38 in 2009 (Fig. 1 (d)). The rising trend rate of FVC was 0.05%/a, which was

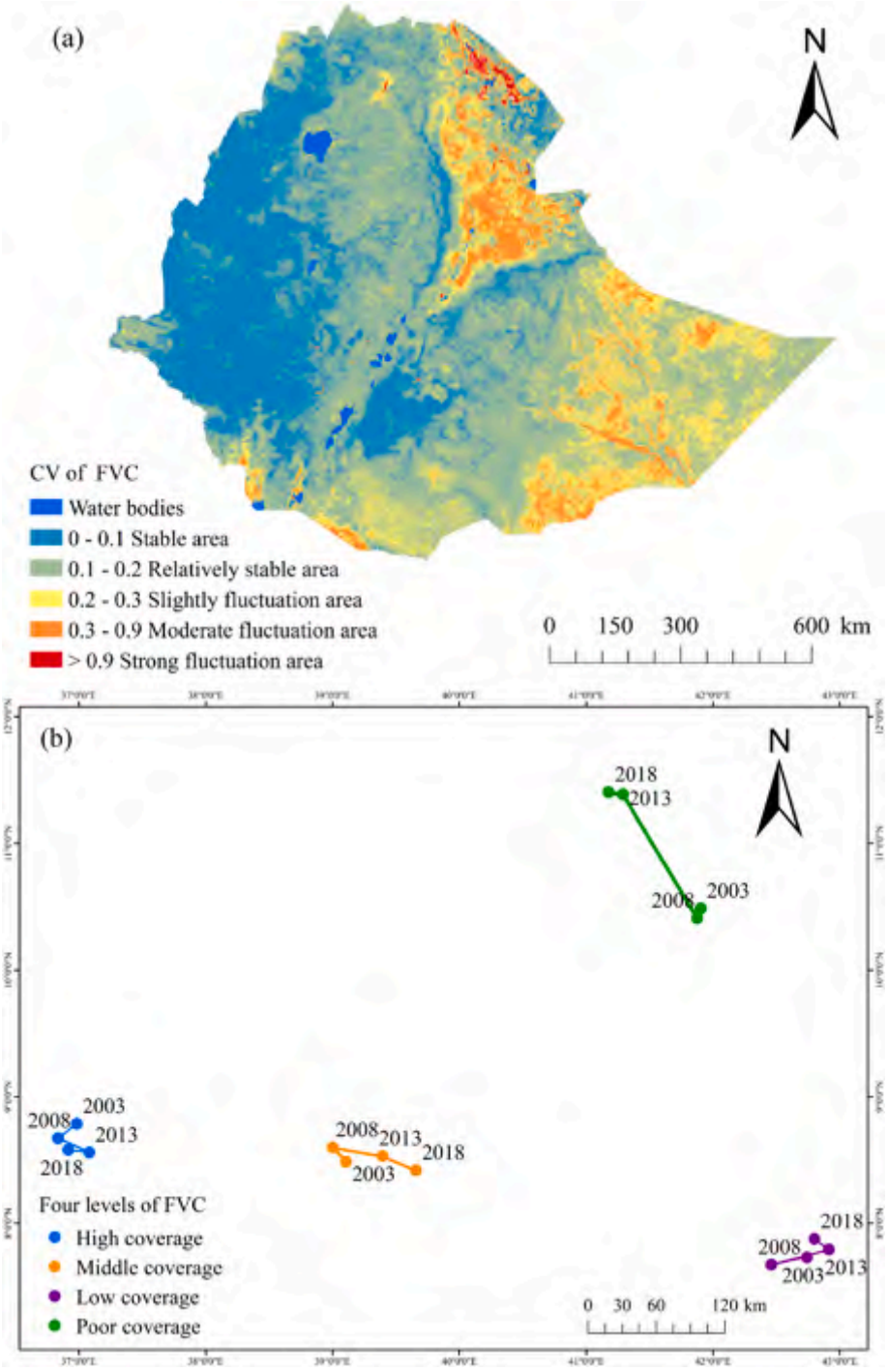

Fig. 3. CV (a), migration trajectory (b), Sen's slope and MK test (c) of FVC in Ethiopia during 2003–2018.

similar to the interannual trend of the EVI. During the period 2003–2018, the FVC generally went through a process of "greening – browning – greening – browning". The change points also reflected this process. As shown in Fig. S2, poor coverage was mainly distributed in the Afar State, showing a trend of first browning and then greening. In 2003, the poor coverage was 123,000 km^2, accounting for 11.25% of the total area. In 2018, the ratio was 9.06%, with a total decrease of 22,900 km^2. The low coverage was mainly distributed in southeastern Ethiopia, showing a trend of first greening and then browning. The middle coverage was mainly distributed in the central part of the study area. In 2018, the middle coverage was 380,000 km^2, accounting for approximately 36% of the study area. Ethiopian croplands were mainly distributed in central and northwestern Ethiopia, which are important parts of middle coverage. High coverage was distributed in the western parts of the study area, showing "browning – greening – browning" trends.

3.2.3. *Trends of vegetation change in Ethiopia during 2003–2018*

The overall variation in the rate of FVC ranged from −3.8%/a to 4%/a (Fig. 3 (c)). The area of FVC decrease and increase accounted for 43.9% and 56.1% of the total area, respectively. Ethiopia was divided into several climatic zones (Viste et al., 2013), among which the contribution

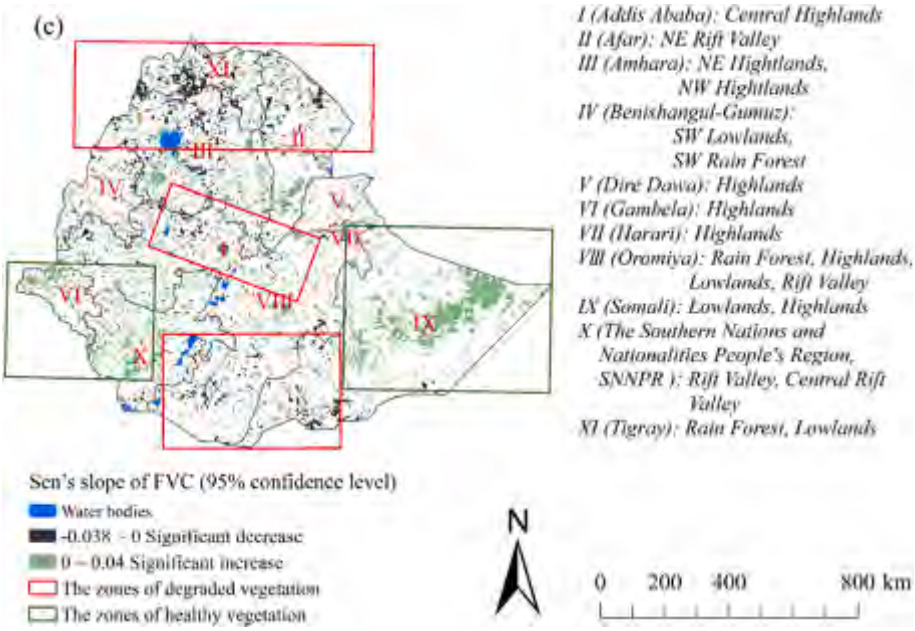

Fig. 3. (*continued*).

rates of driving factors were different, resulting in the obvious spatial heterogeneity of vegetation cover change. The area of significant change in FVC was 110,000 km^2, accounting for approximately 18.87% of the total area. A total of 7.51% of the area decreased in FVC significantly, while 11.36% increased significantly. Although the significant greening was larger than the significant browning in the study area, the comparison between the magnitude of the changing trend and the change area (the number of grids) could infer that there were different degrees of vegetation degradation (Table 1). In zones I, III, IV, VII, and XI, the significantly decreased area of FVC was larger than the significantly increased area. Areas of significant change mainly showed a banded distribution, but sporadic distribution also existed. The areas with FVC significantly reduced were considered as degraded areas, and the areas with FVC significantly increased indicated relatively better vegetation growth. Thus, the main zones of degraded and healthy vegetation could be identified in Ethiopia, with three degraded vegetation zones distributed in the southern, northern, and central parts and two healthy vegetation zones distributed in the southeastern and western parts of the study area. The northern degraded vegetation zone consists mainly of Tigray, Amhara, Afar, and Benshangul oblasts. The central and southern degraded vegetation zone includes the main part of the Oromia region and the capital (Addis Ababa) and the southwest part of Somali state. The western healthy vegetation zone mainly includes the Southern Nations and Nationalities People's Region (SNNPR) and Gambela. The eastern healthy vegetation zone mainly consists of most of the Somali.

Table 1
Comparison of changes in FVC in Ethiopia during 2003–2018.

	Zone I	Zone II	Zone III	Zone IV	Zone V	Zone VI
	The number of grids (FVC change range)					
Decrease	9 (0, 0.0169)	414 (0, 0.0312)	977 (0, 0.028)	101 (0, 0.0179)	3 (0, 0.0089)	24 (0, 0.0164)
Increase	1 (0, 0.0064)	475 (0, 0.0298)	769 (0, 0.02087)	99 (0, 0.0119)	5 (0, 0.005)	348 (0, 0.0201)
	Zone VII	Zone VII	Zone IX	Zone X	Zone XI	–
	The number of grids (FVC change range)					
Decrease	2 (0, 0.0102)	683 (0, 0.0201)	460 (0, 0.0223)	226 (0, 0.0297)	396 (0, 0.0171)	–
Increase	1 (0, 0.006)	590 (0, 0.0274)	2023 (0, 0.0325)	778 (0, 0.0268)	206 (0, 0.012)	–

Note: 95% confidence level.

3.3. Driving factors of vegetation cover

3.3.1. Spatiotemporal characteristics of temperature and precipitation

The mean maximum temperature was >35 °C in the northeastern parts of Ethiopia and the lowlands below 500 m above sea level in the southeastern Somali during 2003 to 2018 (Fig. 4 (a)). In the central highland zone, the temperature continuously decreased with increasing altitude. The mean precipitation was >1550 mm in the western highlands of the study area, but in the central highland region, the precipitation was <1350 mm. In the Afar and Somali regions, where the elevation was generally lower, the precipitation was mostly <350 mm (Fig. 4 (b)), indicating the complexity and unevenness of the spatial distribution of precipitation in Ethiopia. We found that the maximum temperature increase rate was 0.0083 °C/a, and the precipitation increase rate was 6.73 mm/a in Ethiopia. The maximum temperature deviated greatly in 2009 and 2015 due to the high-intensity El Niño. In particular, the precipitation fluctuated greatly. The precipitation in 2003 and 2009 was relatively low. In 2013, the precipitation reached its maximum and then showed a decreasing trend.

3.3.2. Interrelationship between FVC and climate factors

The time lag analysis showed that there was no time lag between EVI and temperature, while there was one month time lag between EVI and precipitation (Table 2). The correlation analysis took into account the time lag of vegetation coverage on climate variables.

The distribution of the correlation between FVC and the MAMaxTemp was substantially spatially heterogeneous (Fig. 5 (a)). The areas with the higher correlation were mainly located in the central highlands of Ethiopia and the border areas of Afar, Oromiya, and Somali. In central Ethiopia at high altitudes (>2000 m), temperature has played an important positive role in the growth and maintenance of local dense vegetation. We found that the MAMaxTemp in these regions was mainly positively correlated with FVC. In the border area of the Afar, Oromiya, and Somali regions, there was a negative correlation between MAMaxTemp and FVC. The results showed that the areas of negative and positive correlations between MAMaxTemp and FVC accounted for 60.14% and 39.86% of the total area, respectively. The area that passed the $p <$

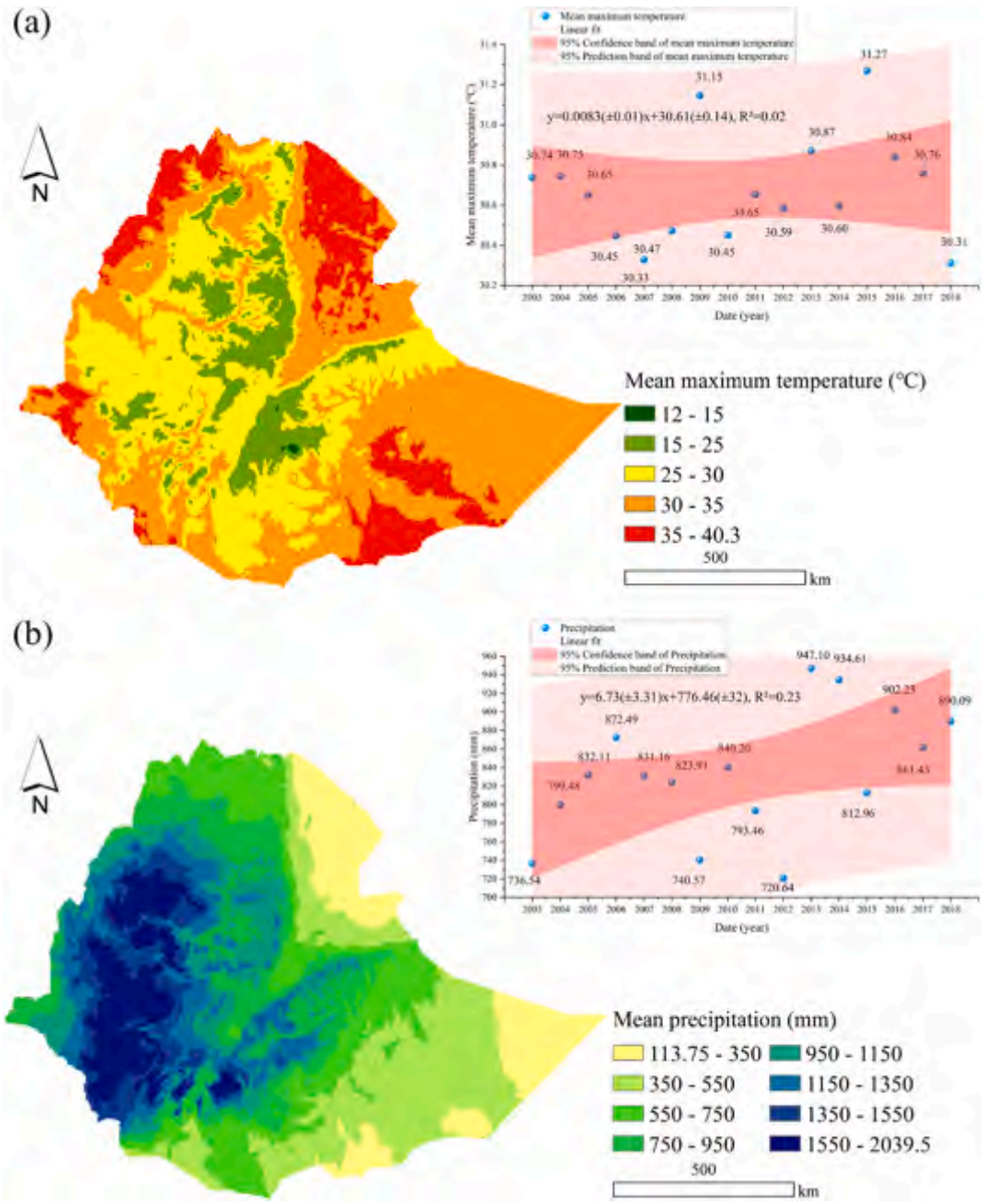

Fig. 4. The spatiotemporal distribution of mean maximum temperature (a) and mean precipitation (b) in Ethiopia from 2003 to 2018.

Table 2
Correlation coefficients between the EVI and climate variables.

$Temp_{lag0}$	$Temp_{lag1}$	$Temp_{lag2}$	$Temp_{lag3}$	$Temp_{lag4}$	$Temp_{lag5}$
−0.72**	−0.51**	−0.18**	−0.15*	0.48**	0.68**
Ppt_{lag0}	Ppt_{lag1}	Ppt_{lag2}	Ppt_{lag3}	Ppt_{lag4}	Ppt_{lag5}
0.70**	**0.88****	0.76**	0.44**	0.02	−0.38**

Note: $Temp_{lagi}$ and Ppt_{lagi} denote the maximum temperature and precipitation with a lag time of i months, respectively; **, highly significant correlation ($p < 0.01$); *, significant correlation ($p < 0.05$).

0.05 significance test was approximately 76,000 km^2, accounting for 6.6% of the total area. The positive correlation between FVC and MAPpt reflected that the areas with the higher correlation values were mainly located in the central-east, southeast, and southwest (the southwest of the SNNPR) of Ethiopia (Fig. 5 (b)). The lower precipitation may contribute to the dependence of vegetation growth on precipitation, thus showing a regional clustering of positive correlations. Excessive precipitation may lead to the oversaturation of vegetation growth, thus showing a scenario wherein negative correlations were distributed. When vegetation is oversaturated with precipitation demand, it may lead to lower radiation and temperature flood disasters, thus limiting the growth of vegetation (Nemani et al., 2003). The area of positive correlation between FVC and MAPpt was 63.01% of the total area, and the area of negative correlation accounted for 36.99%. The area that passed the significance test was 7.87% of the total area, which was mostly positively correlated. The correlation area between FVC and MAPpt passing the significance test was greater than that with temperature, indicating that the effect of precipitation on vegetation cover in the study area was greater than that of temperature.

The regions with the higher correlation between FVC and MMMaxTemp were distributed in central-eastern, southwestern (dominated by

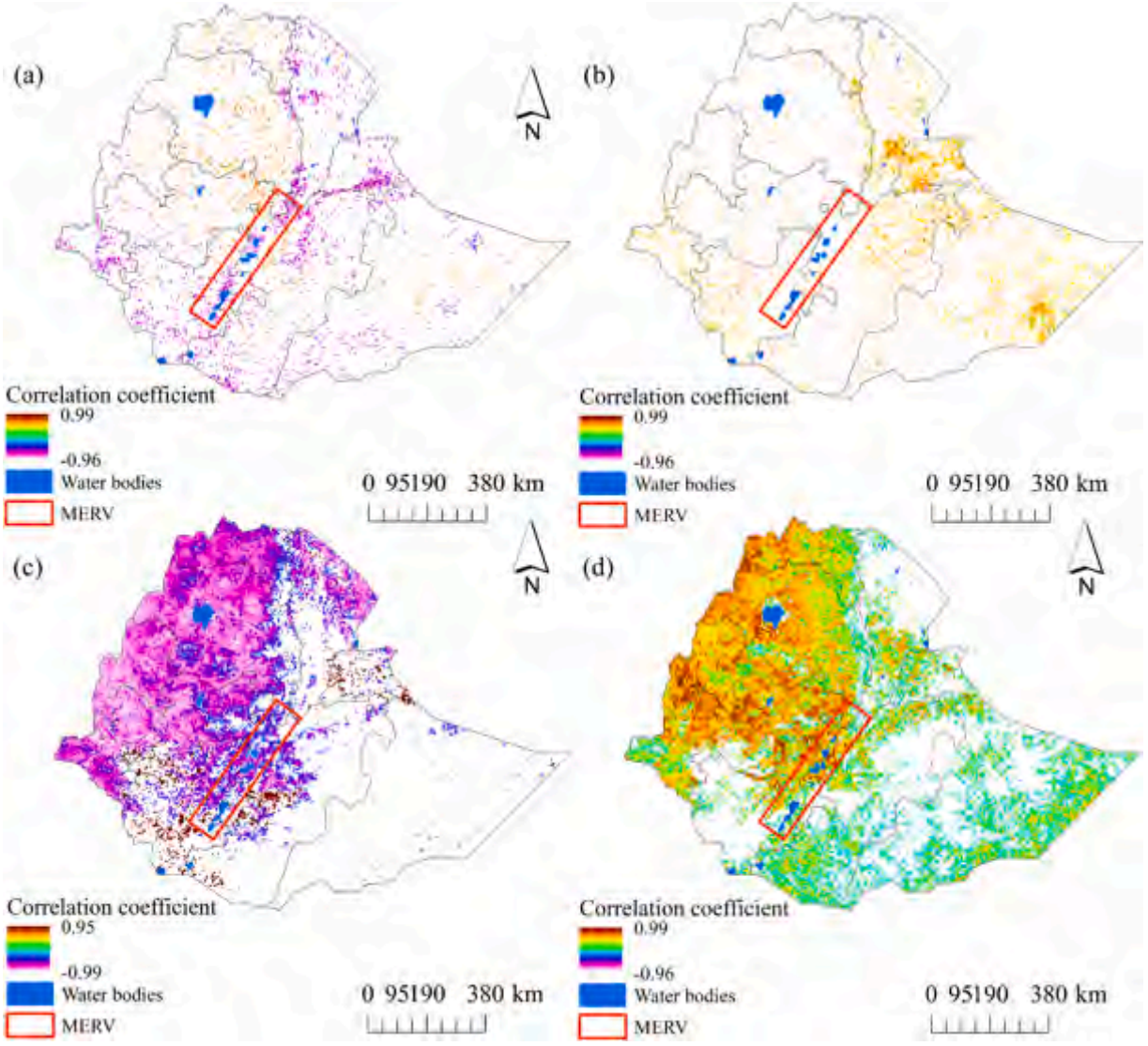

Fig. 5. Correlation distribution between FVC and MAMaxTemp ($p < 0.05$) (a); correlation distribution between FVC and MAPpt ($p < 0.05$) (b); Correlation distribution between FVC and MMMaxTemp ($p < 0.05$) (c); correlation distribution between FVC and MMPpt ($p < 0.05$) (d). Notes: the colorless part of the layer is the area that fails to pass the significance test of $p < 0.05$. MERV is the Main Ethiopian Rift Valley (Omenda, 2007).

the SNNPR), and northwestern Ethiopia (Fig. 5 (c)). Positive and negative correlations dominated in different regions with large spatial differences. Negative correlations predominated in the northwest, while positive correlations were in the southeast. The correlation area that passed the significance test of $p < 0.05$ was 480,000 km^2 and was mainly distributed in the northwest and north-central areas, of which 39.67% was negatively correlated and 2.24% was positively correlated. This indicated that the correlation between FVC and MMMaxTemp was dominated by a significant negative correlation. From Fig. 6 (d), FVC was positively correlated with MMPpt in most areas, while it was negatively correlated in parts of the SNNPR and Afar state. The area that passed the $p < 0.05$ significance test was 58.4% of the total area, in which the positive correlation was predominant. Comparing the regions that passed the significance test, it was found that FVC in the northwest of the Main Ethiopian Rift Valley (MERV) was mainly affected by maximum temperature and precipitation, while the southeastern side of MERV was mainly affected by precipitation.

3.3.3. *Impact of human activities on FVC*

Fig. 6 (a) shows that the negative values of FVC residuals accounted for 45.87% of the total area and were mainly distributed in northern and eastern Afar, southern and southwestern Oromiya, and southwestern Somali. The positive values of FVC residuals accounted for 54.13% of the total area. However, most of the residual trends in the study area did not pass the 0.05 significance test. The area that passed the 0.05 significance test was 129,000 km^2, showing a "scattered overall and concentrated locally" pattern (Fig. 6 (b)). The eastern and northern parts of Ethiopia were locally concentrated areas, and the central part was locally dispersed. In the southeastern and western regions of Ethiopia, the impact of human activities on vegetation cover was continuing to increase. In the south and north, the negative impact of human activities on vegetation cover might continue to increase. The areas that passed the significance test reflected that the impact of human activities on vegetation cover was more frequent in the region. By classifying these areas as zones A–E and by spatial overlay comparing them with degraded vegetation zones and healthy vegetation zones (Fig. 3 (c)), it can be concluded that zones A–E were mainly driven by human activities (Fig. 6 (c)). In particular, the increase in FVC in zones A and C may be related to the increased positive impact driven by human activities, while the decrease of FVC in zones B, D, E may be related to the weakening of the positive impact driven by human activities.

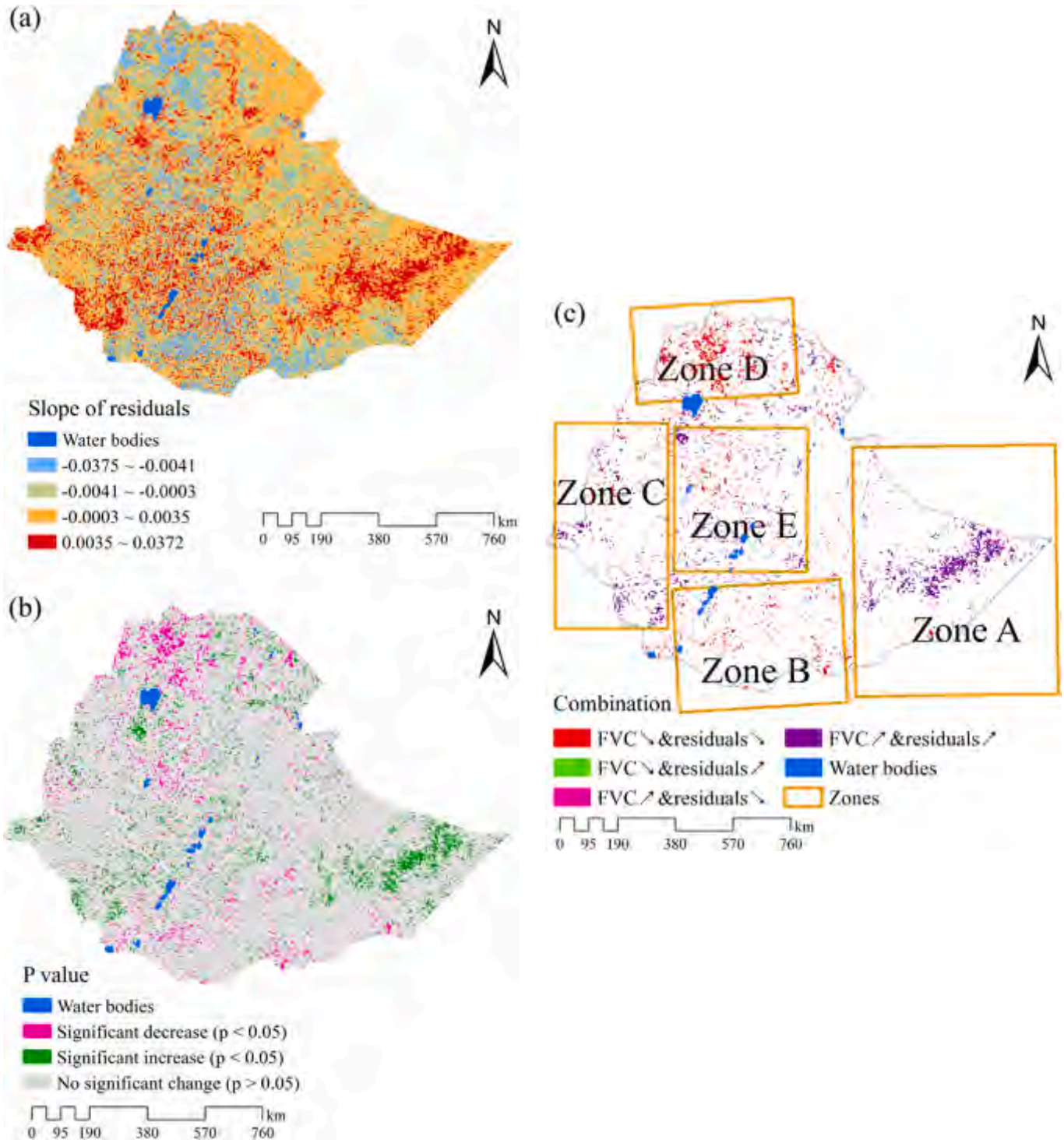

Fig. 6. Slope (a) and significance test (b) of residuals during 2003–2018 ($p < 0.05$), and the different change combinations of residuals and FVC in Ethiopia's degraded and healthy vegetation zones (c).

4. Discussion

4.1. Spatial heterogeneity of driving factors

The correlation between FVC and precipitation was found to be potentially influenced by specific vegetation types, microtopographic landforms, and other features (Ghebrezgabher et al., 2020). Our study showed that not only was the correlation between precipitation and temperature distribution and vegetation cover spatially heterogeneous but also that the influence of human activities on vegetation cover varied from place to place. This indicated that the dominance of climate change and human activities affecting vegetation cover might vary in different regions (Huang et al., 2020). And further, differences in vegetation habitats due to topography in different latitudinal zones have created uniqueness in the spatial and temporal distribution of vegetation changes and the interaction of influencing factors. For example, the dominant climatic (precipitation and temperature) influences on vegetation differ between the southeastern and northwestern regions of

MERV, which may be related to local slopes, slope orientation, and solar irradiance (Muluneh et al., 2017). The northeastern part of the study area is sparsely vegetated, dominated by poor vegetation cover, and has a low population distribution (Hurni et al., 2019). However, the variation coefficient of FVC in this regions was the largest (Fig. 3 (a)), and its center of gravity had the longest migration trajectory (Fig. 3 (b)). This indicated that the lower the vegetation cover, the more fragile the ecosystem is and the more vulnerable it is to external disturbances.

4.2. How do human activities and climate change deepen the impact on vegetation cover?

Studying the effects of climate change and human activities on vegetation cover helps us to improve our understanding of ecosystem vulnerability (Zhao et al., 2018). The FVC in southern and northern Ethiopia showed a significant downward trend, which was regarded as vegetation degradation areas (Fig. 3 (c)). These areas were dominated by high and middle coverage, and the negative impact of human activities on vegetation cover may continuously increase, which should be a key zone for ecological regulation and protection in the future. Insufficient arable land per capita has led to a high dependence on logging and livestock for economic development and farmers' livelihoods (Fao, 2017; Nzabarinda et al., 2021). Livestock farming accounts for 40% of agricultural GDP in Ethiopia (Aleme and Lemma, 2015). Urban expansion, domestic migration, and rapid population growth are important factors of vegetation cover change caused by human activities (Hermans-Neumann et al., 2017). Urban expansion encroached on natural vegetation areas (De La Barrera and Henríquez, 2017) and accelerated land-use turnover. Population pressure inevitably leads to increased overgrazing and indiscriminate logging (Busch and Ferretti-Gallon, 2020). For example, in the northwestern part of Ethiopia, the FVC showed large degradation mainly due to resettlement and agricultural land expansion (Alemu et al., 2015). In the northern highlands of Ethiopia, the change in forest cover was mainly caused by the increase in population and charcoal demand (Belayneh et al., 2020). The ways in which human activities affect vegetation cover also include agricultural practices and invasive alien species. In the Afar State, FVC changes were mainly related to climate change and human activities, in addition to topographic heterogeneity. The uncontrolled growth of exotic species as one of the manifestations of human activities has led to ecosystem vulnerability and sensitivity (Mehari, 2015; Shiferaw et al., 2019).

Climate change mainly affects vegetation growth through extreme temperature and precipitation (Liu et al., 2021; Xiong et al., 2021). extreme temperatures and the lack of precipitation are not conducive to the metabolism of vegetation, leading to the death of vegetation or changes in its growth conditions to adapt to the climatic environment (Li et al., 2018). The interrelationship between vegetation conditions and precipitation in the natural ecosystem of Ethiopia is largely similar to that of western China, i.e., vegetation conditions were positively correlated with precipitation in most arid areas, while they were negatively correlated with precipitation in humid areas (Wang et al., 2015). Further, we found the precipitation in summer and autumn was similar, both of which were >300 mm. It may be related to the Ethiopian climate being controlled by the intertropical convergence zone (ITCZ) (Asefa et al., 2020). The time-series changes in the VIs provided in this paper corresponded to severe climatic anomalies that occur locally or over large parts of the country (Gebrehiwot et al., 2011), mainly manifested by the El Niño and Southern Oscillation (ENSO) (Bayable et al., 2021). ENSO usually leads to drought and uneven or reduced precipitation (Mahmoud and Gan, 2020; Yan et al., 2021), and aggravate the destruction of vegetation (Lanckriet et al., 2015). Until now, the study area presented a continuous warming trend and extremely complex climate changes (Shuai et al., 2018). The frequent occurrence of ENSO is very likely to cause the mass death of vegetation and humans (Berenguer et al., 2021; Fearnside, 2013). For example, affected by ENSO in 2015, large-scale insufficient precipitation occurred in northern and central Ethiopia, causing millions of people to fall into trouble (Philip et al., 2018). Extreme temperatures and precipitation deficits lead to land degradation and the destruction of vegetation growing conditions, which can increase the burden on farmers' livelihoods and in turn may force them to increase deforestation and farmland reclamation for survival. It was evident that the vegetation ecosystem in Ethiopia was deeply affected by climate change and human activities (Tolessa et al., 2020). However, in this paper, the significant correlation area of annual-scale precipitation and maximum temperature on FVC was <10% of the total area, indicating that the influence of climatic factors on FVC was limited. The RESTREND results showed that human activities were the most critical factor contributing to vegetation cover degradation.

4.3. Uncertainty analysis

Based on the characteristics of vegetation cover changes at different time scales, this paper analyzed the overall change trends of vegetation cover across the country and their potential relationship with influencing factors. Similar to other national-scale remote sensing studies, the accuracy of the data limits the precision of the results. In this paper, the resolution of climate data is lower than that of EVI, and the time series data are obtained from the mean values of all rasters, which may affect the accuracy of the final analysis results. In addition, the classification of FVC (high, middle, low, and poor) was mainly verified with the help of the Google Earth Pro platform and land use data, rather than field measurement data, which may cause uncertainty problems. The potential drivers of vegetation cover are broad and complex. The time lags of different vegetation cover types (agricultural land, grassland, forest, etc.) to climate factors may differ, as well as their resilience after exposure to climate change and human disturbance. Future work should consider the interaction of more factor variables and multiple vegetation cover types. Despite the aforementioned uncertainty in this study, the results are still of great positive significance for understanding the basic characteristics of vegetation growth, the influencing factors of spatio-temporal trends of vegetation cover in Ethiopia, and deepening the global public awareness of vegetation cover drivers, which can provide scientific support for ecological restoration and vegetation management.

5. Conclusions

In this paper, we revealed the dynamic change characteristics of vegetation cover in Ethiopia at different time scales by EVI and FVC. Meanwhile, correlation and RESTREND analysis methods were performed to provide insight into the effects of climate factors and human activities on vegetation change. The main findings are as follows.

(1) The FVC of Ethiopia showed an overall increasing trend. In terms of spatial distribution, the quarterly and monthly variations were greater than the interannual variations. The EVI gradually decreased from northwest to southeast, with obvious spatial heterogeneity. The EVI fluctuated irregularly in a sawtooth pattern in the time series. The monthly variation in the EVI was mainly characterized by the “double peaks” pattern.
(2) The vegetation cover in Ethiopia is at risk of local degradation. Spatially, the area of significant browning in FVC was 7.51%, which was lower than the area of significant greening. However, in Addis Ababa, Afar, Amhara, Benishangul-Gumuz, Harari, SNNPR, and Tigray, the trend of significant browning was stronger than significant greening. In Addis Ababa, Amhara, Benishangul-Gumuz, Oromiya, and Tigray, the significant browning was greater than the significant greening.
(3) The effects of climate factors and human activities on FVC had obvious spatial heterogeneity. Among them, human activities were a key factor in the browning of vegetation. In southern, northern, and central Ethiopia, the negative impact of human activities on FVC likely continued to increase, and the positive

impact of local governments on vegetation cover through management policies was weakened. It is crucial to enhance the protection efficiency of vegetation cover in these areas.

Declaration of Competing Interest

The authors declare that they have no known competing financial interests or personal relationships that could have appeared to influence the work reported in this paper.

Data availability

Data will be made available on request.

Acknowledgements

This work was supported by the National Natural Science Foundation of China (Nos. 41761144053, 71761147001), the National Key Research and Development Program of China (No. 2019YFC1407803), and the Big International Science Program of Chinese Academy of Sciences (121311KYSB20190029). We would thank the anonymous reviewers for their valuable suggestions to improve the quality of this paper.

Appendix A. Supplementary data

Supplementary data to this article can be found online at https://doi.org/10.1016/j.ecoinf.2022.101776.

References

Abatzoglou, J.T., Dobrowski, S.Z., Parks, S.A., Hegewisch, K.C., 2018. TerraClimate, a high-resolution global dataset of monthly climate and climatic water balance from 1958–2015. Sci. Data 5, 1–12. https://doi.org/10.1038/sdata.2017.191.

Abera, A., Yirgu, T., Uncha, A., 2020. Impact of resettlement scheme on vegetation cover and its implications on conservation in Chewaka district of Ethiopia. Environ. Syst. Res. 9 https://doi.org/10.1186/s40068-020-00164-7.

Adem, M., Negasi, S., Moghaddam, S.M., Ozunu, A., Azadi, H., 2020. The nexus of economic growth and environmental degradation in Ethiopia: time series analysis. Clim. Dev. 1–12. https://doi.org/10.1080/17565529.2020.1711699.

Aleme, A., Lemma, Z., 2015. Contribution of livestock sector in Ethiopian economy. Rev. Adv. Life Sci. Technol. 29.

Alemu, B., Garedew, E., Eshetu, Z., Kassa, H., 2015. Land use and land cover changes and associated driving forces in north western lowlands of Ethiopia. Int. Res. J. Agric. Sci. Soil Sci. 5, 28–44. https://doi.org/10.14303/irjas.2014.063.

Amsalu, A., Gebremichael, D., 2010. An overview of climate change impacts and responses in Ethiopia in 2009. In: Forum for Environment. Addis Ababa, Ethiopia.

Arneth, A., 2015. Uncertain future for vegetation cover. Nature 524, 44–45. https://doi.org/10.1038/524044a.

Arsiso, B.K., Tsidu, G.M., Stoffberg, G.H., Tadesse, T., 2018. Influence of urbanization-driven land use/cover change on climate: the case of Addis Ababa, Ethiopia. Phys. Chem. Earth Parts A/B/C 105, 212–223. https://doi.org/10.1016/j.pce.2018.02.009.

Asefa, M., Cao, M., He, Y., Mekonnen, E., Song, X., Yang, J., 2020. Ethiopian vegetation types, climate and topography. Plant Divers. 42, 302–311. https://doi.org/10.1016/j.pld.2020.04.004.

Bayable, G., Amare, G., Alemu, G., Gashaw, T., 2021. Spatiotemporal variability and trends of rainfall and its association with Pacific Ocean Sea surface temperature in West Harerge Zone, Eastern Ethiopia. Environ. Syst. Res. 10, 1–21. https://doi.org/10.1186/s40068-020-00216-y.

Belayneh, Y., Ru, G., Guadie, A., Teffera, Z.L., Tsega, M., 2020. Forest cover change and its driving forces in Fagita Lekoma District, Ethiopia. J. For. Res. 31, 1567–1582. https://doi.org/10.1007/s11676-018-0838-8.

Berenguer, E., Lennox, G.D., Ferreira, J., Malhi, Y., Aragão, L.E., Barreto, J.R., et al., 2021. Tracking the impacts of El Niño drought and fire in human-modified Amazonian forests. Proc. Natl. Acad. Sci. 118 https://doi.org/10.1073/pnas.2019377118.

Beyene, S., 2015. Ethiopia's Second National Communication to the United Nation S Framework Convention on Climate Change (UNFCCC). Ministry of Environment an d Forest, Ethiopia.

Busch, J., Ferretti-Gallon, K., 2020. What drives deforestation and what stops it? A meta-analysis. Rev. Environ. Econ. Policy. https://doi.org/10.1093/reep/rew013.

Cannone, N., Guglielmin, M., Malfasi, F., Hubberten, H.W., Wagner, D., 2021. Rapid soil and vegetation changes at regional scale in continental Antarctica. Geoderma 394, 115017. https://doi.org/10.1016/j.geoderma.2021.115017.

Cao, D., Zhang, J., Xun, L., Yang, S., Wang, J., Yao, F., 2021. Spatiotemporal variations of global terrestrial vegetation climate potential productivity under climate change. Sci. Total Environ. 770, 145320 https://doi.org/10.1016/j.scitotenv.2021.145320.

De la Barrera, F., Henríquez, C., 2017. Vegetation cover change in growing urban agglomerations in Chile. Ecol. Indic. 81, 265–273. https://doi.org/10.1016/j.ecolind.2017.05.067.

Dutta, D., Das, P.K., Paul, S., Sharma, J.R., Dadhwal, V.K., 2015. Assessment of ecological disturbance in the mangrove forest of Sundarbans caused by cyclones using MODIS time-series data (2001–2011). Nat. Hazards 79, 775–790. https://doi.org/10.1007/s11069-015-1872-x.

Ebrahimi Khusfi, Z., Zarei, M., 2020. Relationships between meteorological drought and vegetation degradation using satellite and climatic data in a semi-arid environment in Markazi Province, Iran. J. Rangeland Sci. 10, 204–216.

FAO, 2017. Food and Agricultural Organization of the United Nations, FAOSTAT Statistics Database, Food Balance Sheets.

Fearnside, P.M., 2013. Climate change as a threat to Brazil's Amazon forest. Int. J. Soc. Ecol. Sustain. Dev. (IJSESD) 4, 1–12. https://doi.org/10.4018/jsesd.2013070101.

Feng, D., Yang, C., Fu, M., Wang, J., Zhang, M., Sun, Y., et al., 2020. Do anthropogenic factors affect the improvement of vegetation cover in resource-based region? J. Clean. Prod. 271, 122705 https://doi.org/10.1016/j.jclepro.2020.122705.

Fu, X., Shen, Y., Dong, R., Deng, H., Wu, G., 2016. Analysis of urbanization based on center-of-gravity movement and characteristics in Songhua River basin of China and its southern source sub-basin between 1990 and 2010. Chin. Geogr. Sci. 26, 117–128. https://doi.org/10.1007/s11769-015-0757-y.

Funk, C., Hoell, A., Shukla, S., Husak, G., Michaelsen, J., 2016. The East African monsoon system: Seasonal climatologies and recent variations. In: The Monsoons and Climate Change. Springer, pp. 163–185.

Gao, L., Wang, X., Johnson, B.A., Tian, Q., Wang, Y., Verrelst, J., et al., 2020. Remote sensing algorithms for estimation of fractional vegetation cover using pure vegetation index values: a review. ISPRS J. Photogramm. Remote Sens. 159, 364–377. https://doi.org/10.1016/j.isprsjprs.2019.11.018.

Ge, W., Deng, L., Wang, F., Han, J., 2021. Quantifying the contributions of human activities and climate change to vegetation net primary productivity dynamics in China from 2001 to 2016. Sci. Total Environ. 773, 145648. https://doi.org/10.1016/j.scitotenv.2021.145648.

Gebrehiwot, T., Van der Veen, A., Maathuis, B., 2011. Spatial and temporal assessment of drought in the Northern highlands of Ethiopia. Int. J. Appl. Earth Obs. Geoinf. 13, 309–321. https://doi.org/10.1016/j.jag.2010.12.002.

Gebru, B.M., Lee, W.-K., Khamzina, A., Wang, S.W., Cha, S., Song, C., et al., 2020. Spatiotemporal multi-index analysis of desertification in dry Afromontane forests of northern Ethiopia. Environ. Dev. Sustain. 1–28. https://doi.org/10.1007/s10668-020-00587-3.

Ghebrezgabher, M.G., Yang, T., Yang, X., Sereke, T.E., 2020. Assessment of NDVI variations in responses to climate change in the Horn of Africa. Egypt. J. Remote Sens. Space Sci. https://doi.org/10.1016/j.ejrs.2020.08.003.

Gitelson, A.A., Kaufman, Y.J., Stark, R., Rundquist, D., 2002. Novel algorithms for remote estimation of vegetation fraction. Remote Sens. Environ. 80, 76–87. https://doi.org/10.1016/S0034-4257(01)00289-9.

Guo, W., Liu, H., Wu, X., 2018. Vegetation greening despite weakening coupling between vegetation growth and temperature over the boreal region. J. Geophys. Res. Biogeosci. 123, 2376–2387. https://doi.org/10.1029/2018JG004486.

He, P., Xu, L., Liu, Z., Jing, Y., Zhu, W., 2021. Dynamics of NDVI and its influencing factors in the Chinese Loess Plateau during 2002–2018. Regional Sustain. 2, 36–46. https://doi.org/10.1016/j.regsus.2021.01.002.

Hermans-Neumann, K., Priess, J., Herold, M., 2017. Human migration, climate variability, and land degradation: hotspots of socio-ecological pressure in Ethiopia. Reg. Environ. Chang. 17, 1–14. https://doi.org/10.1007/s10113-017-1108-6.

Holben, B.N., 1986. Characteristics of maximum-value composite images from temporal AVHRR data. Int. J. Remote Sens. 7, 1417–1434. https://doi.org/10.1080/01431168608948945.

Huang, S., Zheng, X., Ma, L., Wang, H., Huang, Q., Leng, G., et al., 2020. Quantitative contribution of climate change and human activities to vegetation cover variations based on GA-SVM model. J. Hydrol. 584, 124687 https://doi.org/10.1016/j.jhydrol.2020.124687.

Hurni, K., Hodel, E., Krauer, J., Gämperli, U., Fries, M., Würsch, L., et al., 2019. Ethiopia Geographic Base Map: Population Distribution 2016. https://doi.org/10.7892/boris.133129.

Jarvis, A., Guevara, E., Reuter, H., Nelson, A., 2008. Hole-Filled SRTM for the Globe: Version 4: Data Grid.

Kendall, M.G., 1948. Rank Correlation Methods. Griffin.

Kumar, A., Jhariya, M., Yadav, D., Banerjee, A., 2017. Vegetation dynamics in Bishrampur collieries of northern Chhattisgarh, India: eco-restoration and management perspectives. Environ. Monit. Assess. 189, 1–29. https://doi.org/10.1007/s10661-017-6086-0.

Lanckriet, S., Rucina, S., Frankl, A., Ritler, A., Gelorini, V., Nyssen, J., 2015. Nonlinear vegetation cover changes in the North Ethiopian highlands: evidence from the Lake Ashenge closed basin. Sci. Total Environ. 536, 996–1006. https://doi.org/10.1016/j.scitotenv.2015.05.122.

Li, F., Chen, W., Zeng, Y., et al., 2014. Improving estimates of grassland fractional vegetation cover based on a pixel dichotomy model: A case study in Inner Mongolia, China[J]. Remote Sens. 6 (6), 4705–4722. https://doi.org/10.3390/rs6064705.

Li, C., Wang, J., Hu, R., Yin, S., Bao, Y., Ayal, D.Y., 2018. Relationship between vegetation change and extreme climate indices on the Inner Mongolia Plateau, China, from 1982 to 2013. Ecol. Indic. 89, 101–109. https://doi.org/10.1016/j.ecolind.2018.01.066.

Li, P., Zhu, D., Wang, Y., Liu, D., 2020. Elevation dependence of drought legacy effects on vegetation greenness over the Tibetan Plateau. Agric. For. Meteorol. 295, 108190 https://doi.org/10.1016/j.agrformet.2020.108190.
Liu, H.Q., Huete, A., 1995. A feedback based modification of the NDVI to minimize canopy background and atmospheric noise. IEEE Trans. Geosci. Remote Sens. 33, 457–465. https://doi.org/10.1109/TGRS.1995.8746027.
Liu, H., Jia, J., Lin, Z., Wang, Z., Gong, H., 2021. Relationship between net primary production and climate change in different vegetation zones based on EEMD detrending–a case study of Northwest China. Ecol. Indic. 122, 107276 https://doi.org/10.1016/j.ecolind.2020.107276.
Mahmoud, S.H., Gan, T.Y., 2020. Multidecadal variability in the Nile River basin hydroclimate controlled by ENSO and Indian Ocean dipole. Sci. Total Environ. 748, 141529 https://doi.org/10.1016/j.scitotenv.2020.141529.
Mann, H.B., 1945. Nonparametric tests against trend. Econometrica 245–259.
Mehari, Z.H., 2015. The invasion of Prosopis juliflora and Afar pastoral livelihoods in the Middle Awash area of Ethiopia. Ecol. Process. 4, 1–9. https://doi.org/10.1186/s13717-015-0039-8.
Miralles, D.G., Demuzere, M., Verhoest, N.E.C., Dorigo, W.A., Papagiannopoulou, C., Decubber, S., et al., 2017. A non-linear data-driven approach to reveal global vegetation sensitivity to climate. In: 2017 9th International Workshop on the Analysis of Multitemporal Remote Sensing Images (MultiTemp), pp. 1–3.
Muluneh, A., van Loon, E., Bewket, W., Keesstra, S., Stroosnijder, L., Burka, A., 2017. Effects of long-term deforestation and remnant forests on rainfall and temperature in the Central Rift Valley of Ethiopia. For. Ecosyst. 4, 1–17. https://doi.org/10.1186/s40663-017-0109-8.
Naeem, S., Zhang, Y., Tian, J., Qamer, F.M., Latif, A., Paul, P.K., 2020. Quantifying the impacts of anthropogenic activities and climate variations on vegetation productivity changes in China from 1985 to 2015. Remote Sens. 12, 1113. https://doi.org/10.3390/rs12071113.
Nemani, R.R., Keeling, C.D., Hashimoto, H., Jolly, W.M., Piper, S.C., Tucker, C.J., et al., 2003. Climate-driven increases in global terrestrial net primary production from 1982 to 1999. Science 300, 1560–1563. https://doi.org/10.1126/science.1082750.
Nzabarinda, V., Bao, A., Xu, W., Uwamahoro, S., Jiang, Z., 2021. Impact of cropland development intensity and expansion on natural vegetation in different African countries. Ecol. Inform. 64, 101359 https://doi.org/10.1016/j.ecoinf.2021.101359.
Omenda, P.A., 2007. The Geothermal Activity of the East African Rift. Short Course II on Surface Exploration for Geothermal Resources, Organized by UNU-GTP and KenGen, at Lake Naivasha, Kenya, pp. 2–17.
Ortiz-Bobea, A., Ault, T.R., Carrillo, C.M., Chambers, R.G., Lobell, D.B., 2021. Anthropogenic climate change has slowed global agricultural productivity growth. Nat. Clim. Chang. 11, 306–312. https://doi.org/10.1038/s41558-021-01000-1.
Palmer, L., 2021. How trees and forests reduce risks from climate change. Nat. Clim. Chang. 1–4. https://doi.org/10.1038/s41558-021-01041-6.
Philip, S., Kew, S.F., Jan van Oldenborgh, G., Otto, F., O'Keefe, S., Haustein, K., et al., 2018. Attribution analysis of the Ethiopian drought of 2015. J. Clim. 31, 2465–2486. https://doi.org/10.1175/JCLI-D-17-0274.1.
Piao, S., Yin, G., Tan, J., Cheng, L., Huang, M., Li, Y., et al., 2015. Detection and attribution of vegetation greening trend in China over the last 30 years. Glob. Chang. Biol. 21, 1601–1609. https://doi.org/10.1111/gcb.12795.
Qiu, B., Zeng, C., Tang, Z., Chen, C., 2013. Characterizing spatiotemporal non-stationarity in vegetation dynamics in China using MODIS EVI dataset. Environ. Monit. Assess. 185, 9019–9035. https://doi.org/10.1007/s10661-013-3231-2.
Remy, C.C., Lavoie, M., Girardin, M.P., Hély, C., Bergeron, Y., Grondin, P., et al., 2017. Wildfire size alters long-term vegetation trajectories in boreal forests of eastern North America. J. Biogeogr. 44, 1268–1279. https://doi.org/10.1111/jbi.12921.
Rouse, J., Haas, R.H., Schell, J.A., Deering, D.W., 1974. Monitoring vegetation systems in the Great Plains with ERTS. NASA Spec. Publ. 351, 309.
Sen, P.K., 1968. Estimates of the regression coefficient based on Kendall's tau. J. Am. Stat. Assoc. 63, 1379–1389. https://doi.org/10.1080/01621459.1968.10480934.
Shen, X., Jiang, M., Lu, X., Liu, X., Liu, B., Zhang, J., et al., 2021. Aboveground biomass and its spatial distribution pattern of herbaceous marsh vegetation in China. Sci. China Earth Sci. 64, 1115–1125. https://doi.org/10.1007/s11430-020-9778-7.
Shi, S., Yu, J., Wang, F., Wang, P., Zhang, Y., Jin, K., 2021. Quantitative contributions of climate change and human activities to vegetation changes over multiple time scales on the Loess Plateau. Sci. Total Environ. 755, 142419 https://doi.org/10.1016/j.scitotenv.2020.142419.
Shiferaw, H., Bewket, W., Alamirew, T., Zeleke, G., Teketay, D., Bekele, K., et al., 2019. Implications of land use/land cover dynamics and Prosopis invasion on ecosystem service values in Afar Region, Ethiopia. Sci. Total Environ. 675, 354–366. https://doi.org/10.1016/j.scitotenv.2019.04.220.
Shuai, S., Fadong, L., Yonglong, L., Khan, K., Jianfang, X., Peifang, L., 2018. Spatio-temporal characteristics of the extreme climate events and their potential effects on crop yield in Ethiopia. J. Resour. Ecol. 9 https://doi.org/10.5814/j.issn.1674-764x.2018.03.009.
Swain, S., Abeysundara, S., Hayhoe, K., Stoner, A.M., 2017. Future changes in summer MODIS-based enhanced vegetation index for the South-Central United States. Ecol. Inform. 41, 64–73. https://doi.org/10.1016/j.ecoinf.2017.07.007.
Thompson, R.S., Anderson, K.H., Pelltier, R.T., Strickland, L.E., Shafer, S.L., Bartlein, P. J., 2021. Assessing the uncertainties in climatic estimates based on vegetation assemblages: examples from modern vegetation assemblages in the American Southwest. Quat. Sci. Rev. 262, 106880 https://doi.org/10.1016/j.quascirev.2021.106880.
Tolessa, T., Dechassa, C., Simane, B., Alamerew, B., Kidane, M., 2020. Land use/land cover dynamics in response to various driving forces in Didessa sub-basin, Ethiopia. GeoJournal 85, 747–760. https://doi.org/10.1007/s10708-019-09990-4.
Viste, E., Korecha, D., Sorteberg, A., 2013. Recent drought and precipitation tendencies in Ethiopia. Theor. Appl. Climatol. 112, 535–551. https://doi.org/10.1007/s00704-012-0746-3.
Wang, J., Wang, K., Zhang, M., Zhang, C., 2015. Impacts of climate change and human activities on vegetation cover in hilly southern China. Ecol. Eng. 81, 451–461. https://doi.org/10.1016/j.ecoleng.2015.04.022.
Wang, R., Yan, F., Wang, Y., 2020. Vegetation growth status and topographic effects in the Pisha sandstone area of China. Remote Sens. 12, 2759. https://doi.org/10.3390/rs12172759.
Wu, D., Wu, H., Zhao, X., Zhou, T., Tang, B., Zhao, W., et al., 2014. Evaluation of spatiotemporal variations of global fractional vegetation cover based on GIMMS NDVI data from 1982 to 2011. Remote Sens. 6, 4217–4239. https://doi.org/10.3390/rs6054217.
Xiong, Q., Xiao, Y., Liang, P., Li, L., Zhang, L., Li, T., et al., 2021. Trends in climate change and human interventions indicate grassland productivity on the Qinghai–Tibetan Plateau from 1980 to 2015. Ecol. Indic. 129, 108010 https://doi.org/10.1016/j.ecolind.2021.108010.
Yan, Y., Mao, K., Shen, X., Cao, M., Xu, T., Guo, Z., et al., 2021. Evaluation of the influence of ENSO on tropical vegetation in long time series using a new indicator. Ecol. Indic. 129, 107872 https://doi.org/10.1016/j.ecolind.2021.107872.
Yang, Q., Wang, T., Chen, H., Wang, Y., 2015. Characteristics of vegetation cover change in Xilin Gol League based on MODIS EVI data. Trans. Chin. Soc. Agric. Eng. 31, 191–198. https://doi.org/10.11975/j.issn.1002-6819.2015.22.026.
Zhang, Y., Gao, J., Liu, L., Wang, Z., Ding, M., Yang, X., 2013. NDVI-based vegetation changes and their responses to climate change from 1982 to 2011: a case study in the Koshi River Basin in the middle Himalayas. Glob. Planet. Chang. 108, 139–148. https://doi.org/10.1016/j.gloplacha.2013.06.012.
Zhang, W., Randall, M., Jensen, M.B., Brandt, M., Wang, Q., Fensholt, R., 2021a. Socio-economic and climatic changes lead to contrasting global urban vegetation trends. Glob. Environ. Chang. 71, 102385 https://doi.org/10.1016/j.ecoinf.2017.07.007.
Zhang, X., Liu, L., Chen, X., Gao, Y., Xie, S., Mi, J., 2021b. GLC_FCS30: global land-cover product with fine classification system at 30 m using time-series Landsat imagery. Earth Syst. Sci. Data 13, 2753–2776. https://doi.org/10.5194/essd-13-2753-2021.
Zhao, A., Zhang, A., Liu, X., Cao, S., 2018. Spatiotemporal changes of normalized difference vegetation index (NDVI) and response to climate extremes and ecological restoration in the Loess Plateau, China. Theor. Appl. Climatol. 132, 555–567. https://doi.org/10.1007/s00704-017-2107-8.
Zhou, T., Shen, W., Qiu, X., Chang, H., Yang, H., Yang, W., 2022. Impact evaluation of a payments for ecosystem services program on vegetation quantity and quality restoration in Inner Mongolia. J. Environ. Manag. 303, 114113.